

Magnetoacoustic resonances in bismuth

A. V. Golik, S. P. Korolyuk, V. I. Beletskii, and V. I. Khotkevich

Institute of Radiophysics, Ukrainian Academy of Sciences

and Khar'kov State University

(Submitted January 23, 1976)

Zh. Eksp. Teor. Fiz. 71, 330-340 (July 1976)

The absorption of longitudinal ultra-sound in bismuth in an oblique magnetic field is investigated. It is shown that in the case of drift motion of the carriers along the sound wave vector \mathbf{k} , the absorption anomalies are due to magnetoacoustic resonances at the limiting sections of the bismuth Fermi surface. The experimental results show that the parameters of the hole energy are well described by a quadratic anisotropic model, whereas the shape of the electron Fermi surface is consistent with an empirical model based on the inversion of data on the de Haas-van Alphen effect. An analysis of the shape of the magnetoacoustic resonance lines shows that "noncollisional" sound wave absorption electrons on the limiting-trajectory can be observed over a broad range of inclination of the magnetic field with respect to the vector \mathbf{k} .

PACS numbers: 72.55.+s, 71.30.Hr

INTRODUCTION

A number of magnetoacoustic resonances and oscillation effects have been discovered and investigated in recent years in studies of the absorption of sound in metals. All these are observed in pure single-crystal metals at low temperatures, when the value of the constant magnetic field H satisfies the inequality

$$1 \ll k r_H \ll k l. \quad (1)$$

Here \mathbf{k} is the wave vector of the sound, r_H is the Larmor radius of the electron orbit in the magnetic field, and l is the mean free path.

Under these conditions, resonance sound absorption is due to groups of "effective" electrons, i. e., those electrons whose trajectories contain the points $\mathbf{k} \cdot \mathbf{v} = \omega$ (\mathbf{v} is the velocity of the electrons on the Fermi surface, ω is the cyclic sound frequency). Near these points, the electrons move in phase with the wave and interact effectively with it. Magnetoacoustic resonances are generated when the characteristic dimension of the electron trajectory is equal to an integral number of wavelengths in the metal, $\lambda = 2\pi/k$. In other words, the anomalies in the sound absorption are "spatial" resonances, and their singularities are associated with one mechanism or another of selection of the effective electrons, which enables us to interpret the different resonance effects.

If the sound is propagated in a direction perpendicular to the magnetic field \mathbf{H} , the mean displacement of the electron along the wave vector \mathbf{k} in one period of precession $T = 2\pi/\Omega$ is equal to zero (Ω is the cyclotron frequency). In the quasistatic range of frequencies

$$\omega \ll \nu, \quad (2)$$

when the variable field of the sound wave can be regarded as static during the time of the free flight $\tau = 1/\nu$, magnetoacoustic oscillations of the "geometric resonance" [1,2] are observed (ν is the frequency of collisions of the electrons). In metals with closed Fermi surfaces, all the electrons are "effective," and averag-

ing over the Fermi surface separates out the electrons with extremal diameters $D = D_{\text{extrem}}$, for which the density of states with a given value of D tends to infinity. In this case, the sound absorption coefficient Γ is a periodic function of D_{extrem} .

In the region of high frequencies

$$\omega \gg \nu \quad (3)$$

the change in the sound field during the time of free flight is important. Under these conditions, the electrons interact most effectively with the sound if they are incident at some instant of time on the equivalent plane of constant phase of the traveling acoustic wave. This leads to the excitation of volume acoustic cyclotron resonance (ACR) in the metal at the multiple frequencies [3,4]

$$\omega = n\Omega, \quad n = 1, 2, 3, \dots \quad (4)$$

The role of the "skin layer" in this case is played by the advancing front of the sound wave. As in electromagnetic cyclotron resonance, ACR is most strongly pronounced when the frequencies Ω are identical for all electrons, i. e., in the case of a quadratic dispersion law. In the case of a nonquadratic dispersion law, the "resonating" electrons have extremal cyclotron masses m_{extrem}^* [5]. The periods of the ACR and magnetoacoustic oscillations of "geometrical resonance" differ by a factor of $v/s \gg 1$ (s is the sound velocity).

Another group of magnetoacoustic resonances is associated with the drift of electrons along the wave vector of the sound \mathbf{k} . [6-9] In the low-frequency region (2), upon satisfaction of the condition

$$|k_H \bar{v}_H| = n\Omega, \quad n = 1, 2, 3, \dots \quad (5)$$

the electrons are periodically accelerated by the sound field in the planes of constant phase, where they remain for a relatively longer time than on the remaining portions of the trajectory (k_H and v_H are respectively the projections of the wave vector of the sound \mathbf{k} and the electron velocity vector \mathbf{v} in the direction of the mag-

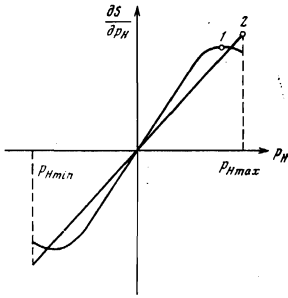


FIG. 1. Dependence of the quantity $\partial S/\partial p_H$ on p_H for an ellipsoidal Fermi surface (straight line) and for a nonellipsoidal Fermi surface, which has a peculiarity in the density of states at $p_H < p_{H \max}$. The points are 1—resonance of density of states, 2—“edge of the Kjeldaas absorption.”

netic field. The bar indicates averaging over the period of rotation T of the electron). The condition (5), rewritten in the form

$$U(p_H) = n\lambda, \quad (6)$$

shows that those electrons interact with the sound in resonance fashion whose displacement $U(p_H)$ is a multiple of the wavelength λ ($U(p_H) = |2\pi\Omega^{-1}\bar{v}_H \cos\theta|$ is the absolute value of the displacement of the electrons along the vector \mathbf{k} in the period T , p_H is the projection of the momentum of the electron on the magnetic field, and θ is the angle between the vectors \mathbf{k} and \mathbf{H}).

In the high frequency region (3), Doppler splitting of the resonance lines is observed, associated with the fact that one-half of the electrons drift along the direction of sound propagation and the other against it. In this case, we need to take into account in Eq. (5) the sound frequency

$$|\omega - k_H \bar{v}_H| = n\Omega. \quad (7)$$

For closed Fermi surfaces, electron drift along the \mathbf{k} vector is possible only for non-perpendicular \mathbf{k} and \mathbf{H} . Resonance is observed on open periodic trajectories also in the case $\mathbf{k} \perp \mathbf{H}$, provided that the wave vector \mathbf{k} is not parallel to the direction of the open trajectory and the angle φ between \mathbf{k} and the direction of the open trajectory is not small, so that $\mathbf{k} \cdot \mathbf{v}T \sim k v_H \sin\varphi \gg 1$.

The variety of magnetoacoustic effects in the presence of electron drift is connected with the character of the dependence of the quantity \bar{v}_H/Ω on p_H . If $U(p_H)$ does not depend on p_H , then the condition (6) is satisfied simultaneously for all electrons. Just this case is realized on open periodic trajectories at $\mathbf{k} \perp \mathbf{H}$,^[7] when the resonance is due to electrons with $U(p_H) = U_{\text{extrem}}$, for which the density of states with given displacement $U(p_H)$ tends to infinity. If the Fermi surface is closed, then the extremum of the displacement $U(p_H)$ is identical with the extremum of the function $\partial S(p_H)/\partial p_H$ ($S(p_H)$ is the area of the orbit with $p_H = \text{const}$).

It is seen from Eq. (6) that for given n there exists a value of the magnetic field $H = H_1$, above which there is no resonance absorption. At $H < H_1$, when the condition (6) is satisfied, the energy of the sound wave is absorbed by electrons with $(\partial S/\partial p_H)_{\text{extrem}}$. The value of $\partial S/\partial p_H$ on ellipsoidal Fermi surfaces is extremal in the vicinity of the elliptic limiting point at $p_H = p_{H \max}$. Since

the electrons near the limiting point are in general not effective in the sense of satisfying the condition $\mathbf{k} \cdot \mathbf{v} \approx 0$, the amplitude of the resonance is small—a break should be observed on the curve of the dependence of the absorption coefficient Γ on the value of the magnetic field.^[6] This effect is known in the literature as the “edge of the Kjeldaas absorption.” If the shape of the Fermi surface is different from ellipsoidal, the function $\partial S/\partial p_H$ can have an extremum even at values of $p_H < p_{H \max}$. Since the resonance sound absorption is, as before, determined by the electrons for which the derivative $\partial S/\partial p_H$ is extremal, and the density of the latter with the given value of $(\partial S/\partial p_H)$ tends to infinite—this case is known as the “resonance density of states.”^[7] Figure 1 shows the difference between the “edge of the Kjeldaas absorption” and the “resonance density of states.”

Finally, the mechanism of selection of the electrons can be connected with the difference in the character of the sound absorption by “effective” and “ineffective” electrons. The projection of the ellipsoidal Fermi surface on the plane of the vectors \mathbf{k} and \mathbf{H} is shown in Fig. 2. The system of vertical lines separates groups of resonance electrons on the Fermi surface with different p_H , which satisfy Eq. (6) for different n . A change in the value of the magnetic field leads to a change in the number of resonance states in the interval $-p_{H \text{gr}} < p_H < p_{H \text{gr}}$ which separates the region of “effective” electrons on the Fermi surface. Anomalies in the absorption appear when the group of resonance electrons crosses the section of the Fermi surface on which they touch the belt $\mathbf{k} \cdot \mathbf{v} = 0$ only once.^[8] We shall call this the boundary section in what follows.

The magnetoacoustic resonance phenomena described above, in the case of drift motion of the carriers along the wave vector of the sound, can give a great deal of information on the singularities of the energy spectrum of the electrons from noncentral parts of the Fermi surface, since the position of the resonance peaks in the magnetic field is determined by the differential character of $\partial S/\partial p_H$. However, the number of experimental researches in which these effects are observed is not large. Magnetoacoustic resonances on the boundary sections have been observed only in antimony^[10,11]; resonances associated with the singularities of the density of states were discovered experimentally in gallium^[12] and tungsten.^[13] Magnetoacoustic resonances on open periodic trajectories have been observed in tin,^[7] cadmium,^[14] copper,^[15] zinc,^[16] thallium^[17] and gallium.^[12] The Fermi surfaces of most metals have a very complicated shape, which makes the interpretation of the experimental results and unambiguous identification of the mechanism of selection of the “reso-

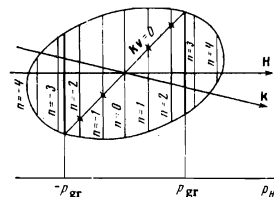


FIG. 2. Projections of the ellipsoidal Fermi surface on the planes of the vectors \mathbf{k} and \mathbf{H} . The vertical lines indicate the resonance states in the range $-p_{H \text{gr}} < p_H < p_{H \text{gr}}$.

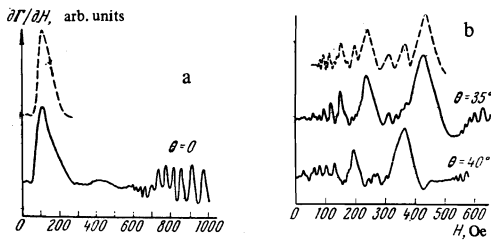


FIG. 3. Example of recording the derivative of the sound absorption coefficient: a) $k \parallel dH \parallel C_1$, b) $k \parallel P_y$, $\theta = 35^\circ$ and $\theta = 40^\circ$ in the plane $P_y C_{33}$. The dashed lines are from the calculation of the shape of the lines of magnetoacoustic resonance according to Eq. (11).

nating" electrons very difficult, especially in the case of a closed Fermi surface. Therefore, we have made an attempt at an experimental observation of magnetoacoustic resonances in the drift of electrons along the k vector and at their unambiguous interpretation in bismuth, the energy spectrum of the carriers of which is sufficiently well known at the present time.^[18-21]

EXPERIMENTAL METHOD

Samples for measurements, of thickness 2 mm and diameter 8 mm, were cut on an electric spark cutter from the bulk single crystal,^[1] which was grown from the melt by the Czochralski method. The orientation of the crystal was established in this case by means of an optical goniometer with a base of 1.5 m and with an accuracy to within 0.1° . The working surfaces of the sample were ground by abrasive powder only to remove traces of scratches and were damaged to a depth of 0.1–0.2 mm. Most of the interior of the sample remained deformation-free under such a treatment. The prepared samples were characterized by a residual resistance $R(300^\circ\text{K})/R(4.2^\circ\text{K}) \approx 400$.

The small amplitude of magnetoacoustic effects in bismuth, the large value of the lattice sound absorption, and the damaged surface of the sample, which worsens the acoustic coupling between the latter with the source and with the sound receiver, have imposed more stringent requirements on the ultrasonic spectrometer. Longitudinal sound of frequency $\omega/2\pi = 500$ MHz was excited and received by means of high-efficiency piezotransducers of lithium niobate with a fundamental resonance frequency of 167 MHz. To decrease the loss in the high-frequency portion of the spectrometer when sound absorption was studied in an oblique magnetic field, low-temperature apparatus was used which permitted us to obtain excellent matching of the piezotransducers with the coaxial line. This apparatus is described in detail in Ref. 22. In the case of mutually perpendicular orientation of the vectors k and H , a modified variant of the high-frequency attachment, described in Ref. 23, was used.

Impedance matching was accomplished here by capacitive impedance transformers located outside the cryostat. These measures made it possible to decrease the high-frequency power transferred to the radiating transducer to several milliwatts, which excluded the possibility of heating the sample. The latter

estimates were made from observations of the Doppler splitting of the lines of magnetoacoustic resonance in antimony.

The low-frequency (narrow band amplifier + phase detector) system usually employed in spectrometers was replaced by a reamplifier + synchronous integrator + phase-detector system, which has much greater null stability, is insensitive to the frequency drift of the reference voltage, and has a wider dynamic range.^[24]

The magnetic field was measured with an accuracy of 0.5% by a Hall pickup calibrated by NMR. The basic constant magnetic field was modulated by a sinusoidal field with amplitude of 10 Oe and frequency 12.5 Hz, which enabled us to record the derivative of the absorption with respect to the magnetic field $\partial\Gamma/\partial H$. For additional adjustment of the sample, we used the "tilt" effect in sound absorption.^[25] The measurements were carried out at 1.6°K.

RESULTS OF MEASUREMENTS

We studied the singularities of the sound absorption at two orientations of the wave vector k relative to the axes of the crystal:

I. The sound wave vector is parallel to the bisector axis C_1 , the magnetic field vector H is rotated in the plane of the trigonal and bisector axes C_3 and C_1 and in the plane of the binary and bisector axes C_2 and C_1 .

II. The sound wave vector is parallel to the major axes P_y of the electron "ellipsoid." The magnetic field vector H is rotated in the planes of the axes $P_y C_3$ and $P_y C_2$.

Figure 3a shows the example of recording the differential sound absorption coefficient $\partial\Gamma/\partial H$ as a function of the magnetic field for orientation I at $k \parallel H$. A maximum of the function $\partial\Gamma/\partial H$ is observed on the curve, connected with the resonance absorption of sound by the electron group of carriers. In a stronger magnetic field, giant quantum oscillations (GQO) are observed, due to the same "ellipsoid." The amplitude of the GQO is small because of the large time constant of the recording apparatus.

For inclinations of the vector H in the planes $C_1 C_2$ and $C_1 C_3$ to the axis C_1 in the range of angles 30 – 60° , there is a group of magnetoacoustic resonances connected with the hole Fermi surface of bismuth. In strong fields, the curve is the superposition of the magnetoacoustic resonances from the hole Fermi surface and the quantum magnetoacoustic oscillations. Near the inclination angle $\theta \approx \pi/2$, oscillations of "geometric resonance," whose amplitude increases sharply at $\theta = \pi/2$, are observed from the electron Fermi surface of bismuth.

The characteristic form of the dependences of $\partial\Gamma/\partial H$ for the orientation II is shown in Fig. 3b. These resonances are due to the hole Fermi surface and are observed in the region of angles of inclination of H of 25 – 65° from the direction of P_y in the planes $P_y C_2$ and $P_y C_3$. At this orientation of the wave vector of the sound, close to $\theta = \pi/2$, oscillations are also observed

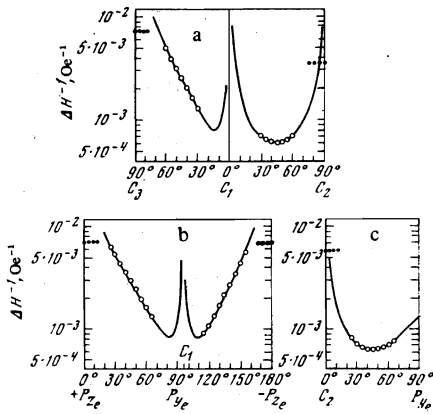


FIG. 4. Anisotropies of the periods of the magnetoacoustic resonances on the hole Fermi surface of bismuth: a)—orientation I, b) and c)—orientation II; ○—periods of magnetoacoustic resonances, ●—periods of the oscillations of the “geometric resonance” on the electron Fermi surface, solid lines—calculation of the periods in the quadratic approximation of the dispersion law.

of the “geometric resonance” from the electron “ellipsoid.” Figures 4 and 5 show the measured periods of the magnetoacoustic resonances and oscillations of the “geometric resonance” for orientations I and II of the sound wave vector.

DISCUSSION OF THE RESULTS

The ultrasonic absorption in semimetals is due to the deformation interaction of the carriers with the sound wave. In bismuth, in propagation of longitudinal sound near the crystallographic axes C_1 , the absolute value of the potential of this interaction is equal to 5.65 eV for the “principal ellipsoid,” the major axis of which, P_y , is inclined at an angle of $6^\circ 20'$ to the C_3 axis from the C_1 axis, and 1.23 eV for the hole surface. For two other electron “ellipsoids,” this value is practically equal to zero,^[26] i. e., at the chosen orientations I and II, of the vector \mathbf{k} , the sound absorption is due to the “principal” electron and hole ellipsoids, which simplifies the analysis of the experimental results.

To prepare a sample of orientation II, it is necessary to determine the directions $+C_3$ and $-C_3$ in the initial single crystal. In ultrasonic investigations, the only dependable possibility for this is the measurement of the periods of oscillation of the “geometric resonance.” Since the period of the oscillations in “geometric resonance” is connected with the extremal dimensions of the Fermi surface in the direction $\mathbf{k} \times \mathbf{H}$ by the relation

$$\Delta H^{-1} = e\lambda/cD_{\text{extrem}} \quad (8)$$

it follows that for $\mathbf{k} \parallel P_y$, the periods of the oscillations at $\mathbf{H} \parallel P_x$ and $\mathbf{H} \parallel P_z$ should differ by a factor of about 1.2. In the case of incorrect orientation of the sample, the angle between \mathbf{k} and P_y would be $12^\circ 40'$ and the periods would differ by a factor of about 3.4. Under these same conditions, the determination of the directions $+C_3$ and $-C_3$ with the help of the GQO requires an accuracy of measurement of the periods to within no

worse than 1%, which represents a rather complex experimental problem. The measured periods of the “geometric resonance” at $\mathbf{H} \parallel P_x$ and $\mathbf{H} \parallel P_z$ are equal to $\Delta H^{-1} = 5.85 \times 10^{-3} \text{ Oe}^{-1}$ and $\Delta H^{-1} = 7.2 \times 10^{-3} \text{ Oe}^{-1}$, respectively, whence, in accord with (8), $p_x = (5.6 \pm 0.1) \times 10^{-22} \text{ g-cm/sec}$; $p_z = (7.4 \pm 0.1) \times 10^{-22} \text{ g-cm/sec}$. If the axis of rotation of the magnetic field is identical with the vector \mathbf{k} , we then can establish the projection of the zone of “effective” electrons with $\mathbf{k} \cdot \mathbf{v} = 0$ on the plane of rotation of the magnetic field from the oscillations of the “geometric resonance.” In such a method of experiment, differences were observed in Ref. 27 between the measured “shadow” projection of the electron Fermi surface of bismuth on the plane C_2C_3 and its ellipsoidal approximation. The results of Ref. 29 and the present communication show that these divergences are connected with the deviation of the real electron Fermi surface of bismuth from an ellipsoid, which is maximal in this plane, and not with the error in the orientation of the sample, as had been proposed earlier. Thus, the ultrasonic measurements of Ref. 27 have first revealed the deviation of the electron Fermi surface of bismuth from ellipsoidal, previously noted in Ref. 18. The “shadow” dimensions, recorded in Ref. 27 for the electron surface in the C_2C_3 plane, agree within 2–3% with those calculated from the data of Ref. 20. The measurements obtained in the present work for the dimensions of the electron Fermi surface of bismuth also agree, within the limits of error of the experiment, with those measured in Ref. 20 and are not cited here.

As had been noted earlier, the magnetoacoustic resonances in the drift motion of the carriers along the wave vector of the sound can be connected either with the singularities of their energy spectrum, or with the change in the number of resonance states in the interval $-\rho_{H \text{ gr}} < \rho_H < \rho_{H \text{ gr}}$, near the limiting point. It was shown in Refs. 18–21 that the shape of the hole Fermi surface in bismuth is well described by the ellipsoidal approximation, which excludes the possibility of observation of magnetoacoustic resonances connected with the singularities of the density of states on the hole Fermi surface. The periods of the magnetoacoustic resonances on the boundary sections in the approximation of the quadratic dispersion law and $\omega \ll \nu$ are connected with

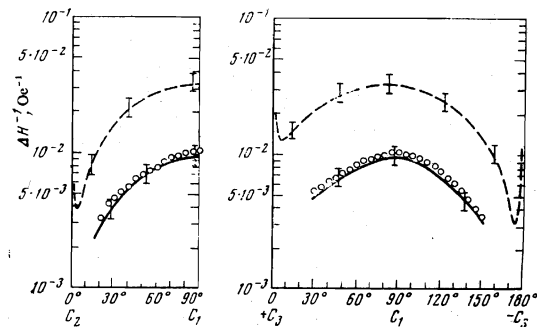


FIG. 5. Anisotropies of the periods of the magnetoacoustic resonances on the electron Fermi surface of bismuth (orientation I), ○—periods of the resonances, dashed curves—quadratic approximation of the dispersion law, solid curves—calculation of the periods from the numerical model.

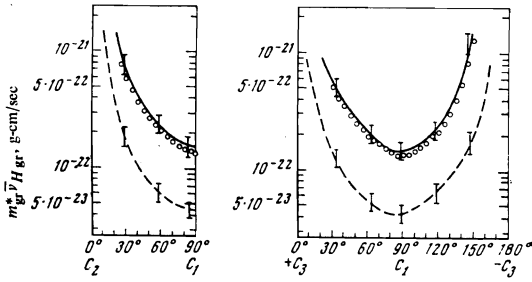


FIG. 6. Anisotropies of the value of $m_{gr}^* \bar{v}_{H gr}$ for the electron Fermi surface of bismuth: \circ —experimental values, dashed curves—quadratic approximation, solid curves—calculation according to the numerical model.

the parameters of the energy spectrum in the following fashion^[9]:

$$\Delta H_{gr}^{-1} = \frac{e\lambda}{2\pi c \cos \theta} \left\{ \frac{2m_0 \varepsilon_F |\hat{m}|}{(h\hat{m})^2} \left[1 - \frac{(h\mathbf{q})^2}{(h\hat{m})(q\hat{m}^{-1}q)} \right] \right\}^{-1}, \quad (9)$$

($\mathbf{q} = \mathbf{k}/|\mathbf{k}|$, $\mathbf{h} = \mathbf{H}/|\mathbf{H}|$, c is the velocity of light, e is the electron charge, ε_F is the Fermi energy, m_0 is the mass of the free electron, and \hat{m} is the tensor of the dimensionless effective masses).

The constants of the spectrum for the calculations were taken from Refs. 18–21. The sound velocity for the direction $\mathbf{k} \parallel C_1$ is equal to $s = 2.70 \times 10^5$ cm/sec.^[26] The curves calculated from Eq. (9) are plotted in Fig. 4 as solid lines. The error in this calculation, which is connected with the possible error in the orientation of the sound wave vector by an angle $\pm 2^\circ$, is equal to ± 3 –5%. The excellent agreement of the experimental results with the calculated values indicates that the deviation of the hole Fermi surface of bismuth from an ellipsoid does not exceed 0.1% according to our results. The relations

$$\Delta H^{-1} = \frac{e\lambda}{c \cos \theta (\partial S / \partial p_H)}, \quad \partial S / \partial p_H = 2\pi m^* \bar{v}_H, \quad (10)$$

which are valid for an arbitrary dispersion law, a special case of which are Eqs. (9), connect the periods of the magnetoacoustic resonances in a magnetic field with the parameters of the current carriers on the boundary trajectories. Since the calculation of all the characteristics of the ellipsoidal Fermi surface does not present any difficulty, the experimental and calculated values of $m_{gr}^* \bar{v}_{H gr}$ on the boundary sections of the hole Fermi surface of bismuth will not be written down here.

The periods of the magnetoacoustic resonances for the "principal" electron "ellipsoid," calculated from Eq. (9), are shown by the dashed curve in Fig. 5. The vertical bars show the range of deviations which could result upon error in the orientation of the sample by an angle of $\pm 2^\circ$, which clearly exceeds the error of adjustment of the crystal in the cryostat. It is seen that the results cannot be explained within the framework of the ellipsoidal Fermi surface. An attempt was therefore made to compare our experimental results with the numerical model of the electron Fermi surface of bis-

moth, based on the inverse of data on the de Haas–van Alphen effect.^[20]

The coefficients of the expansion of the square of the momentum in spherical harmonics in the transformed system of coordinates are given below in units of 10^{-42} $\text{g}^2\text{-cm}^2/\text{sec}^2$:

B_{mn}	B_{00}	B_{20}	B_{21}	B_{22}	B_{40}	B_{41}	B_{42}	B_{43}	B_{44}
Value:	58.8	-3.09	-1.217	-2.04	-2.13	-0.102	-0.212	0.0586	0.01867

The anisotropy of the quantity

$$\left(\frac{\partial S}{\partial p_H} \right)_{gr} = \left| \lim_{\Delta p_H \rightarrow 0} \frac{S_1 - S_2}{\Delta p_H} \right|$$

was found from an empirical model. Here S_1 and S_2 are the areas of the cross sections of the Fermi surface with planes normal to the vector of the magnetic field and passing through the points $p_{H gr}$ and $p_{H gr} + \Delta p_{H gr}$. Since the values of the periods ΔH_{gr}^{-1} and the products $m_{gr}^* \bar{v}_{H gr}$ calculated according to this scheme differed from the experimental values by 20–25%, the possible departures of the numerical model from the real electron Fermi surface of bismuth were taken into account in the limits of the matrix of the coefficients of expansion of the dispersion.^[20] The value of the momentum in the transformed system of coordinates in the quadrant from $+P_y$ to $+P_z$ were put in the form $R_{num}(1 - 8 \times 10^{-3} \sin^2 \varphi)$. Since the boundary sections in our experiments did not include the entire electron Fermi surface, it was not possible to make precise the coefficients of expansion of the square of the momentum in the transformed set of coordinates. The final results are given in Figs. 5 and 6 and are in excellent agreement with experiment. The vertical bars show a similar range of possible errors. Such a significant divergence of the experimental and calculated results from the ellipsoidal approximation is connected with the fact that the point around which the planes of the boundary sections rotate is located at higher momenta p_y in comparison with the ellipsoid, Fig. 7.

In the orientation II, the band of "effective" electrons with $\mathbf{k} \cdot \mathbf{v}$ lies in the plane $P_x P_z$ on the central, almost cylindrical, portion of the electron Fermi surface, where the derivative $(\partial S / \partial p_H)_{gr} \approx 0$. The value of the field of the magnetoacoustic resonance at the boundary section with $\eta = 1$ for this orientation is smaller than 1

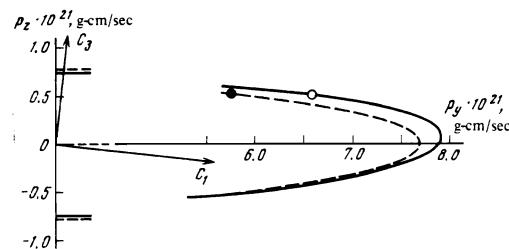


FIG. 7. Form of the electron Fermi surface of bismuth according to Ref. 20. The solid curve is the numerical model, the dashed is the ellipsoidal approximation. The circles indicate $p_{H gr}$, about which the boundary sections rotate: \circ —real electron Fermi surface of bismuth, \bullet —its ellipsoidal approximation.

Oe, which could not be recorded by our experimental method. The absence of resonance from the electron Fermi surface in orientation II of the wave vector \mathbf{k} at coincidence of the directions of the magnetic field in cases I and II confirms the fact that the observed effect is not the "edge of the Kjeldaas absorption," the periods of oscillation of which depend only on the orientation of \mathbf{H} and do not depend on the direction of the sound propagation. Our calculation revealed the absence of an extremum of the function $\partial S/\partial p_H$ at $p_H < p_{H \max}$ for the electron Fermi surface of bismuth in the case of arbitrary orientations of the vector \mathbf{H} . The circumstances indicated above give a basis for asserting that magnetoacoustic resonances on the boundary cross sections were observed in bismuth in our experiments for the first time.

The absorption coefficient of longitudinal sound in the quasistatic region of frequencies has the following form^[9]:

$$\Gamma = \frac{1}{4\pi w |U|^2 \hbar^2} \sum_{\alpha} |\delta \epsilon|^2 \frac{m_0}{\Omega} \sum_{s=-\infty}^{\infty} \int_{-p_{H \max}}^{p_{H \max}} dp_H D \left(s - \frac{\omega}{\Omega} + k_H \rho \frac{p_H}{p_{H \max}} \right) \times J_s^2 [k_H \rho \beta \sqrt{1 - p_H^2/p_{H \max}^2}], \quad (11)$$

$$D \left(s - \frac{\omega}{\Omega} + k_H \rho \frac{p_H}{p_{H \max}} \right) = \frac{\gamma}{\pi [\gamma^2 + (s - \omega/\Omega + k_H \rho p_H/p_{H \max})^2]},$$

$$\beta = [(\hbar m) (\mathbf{q} \hat{m}^{-1} \mathbf{q}) - (\mathbf{q} \hbar)^2]^{1/2}$$

(w is the density of the metal, $|U|$ is the amplitude of the sound wave, $\delta \epsilon$ is the addition to the energy of the electron due to interaction with the sound, $\rho = \bar{v}_H \max / \Omega$, α is the index of the group of carriers of the multi-valley Fermi surface, $\gamma = \nu / \Omega$). The curves of $\partial \Gamma / \partial H$ calculated according to Eq. (11) in the approximation $\gamma \rightarrow 0$ are shown in Fig. 3 by the dashed lines. This approximation is valid even in the case of a finite length of the free path under the condition that the width of the D function $\Delta(p_H/p_{H \max}) \sim (k_H l_H)^{-1}$ is close to its maximum remains smaller than the characteristic smearing of the square of the Bessel functions:

$$\Delta(p_H/p_{H \max}) \ll 6^{1/2} q_H^2 / s^{1/2} \beta \sqrt{\beta^2 + q_H^2}.$$

This circumstance imposes a limitation on the range of angles of inclination of the magnetic field at which such a "collision-free" absorption is observed. Numerical estimates show that at the investigated orientations of the sound, I and II, the "collision-free" region lies in a wide range of values of $k_H \rho$ and goes over into the "collision" region at $k_H \rho < 1$. Experimentally, this is confirmed by the fact that the characteristic width of the lines of magnetoacoustic resonance is smaller than their periods, Fig. 3b. Aperiodic oscillations in the intermediate region between resonant spikes can be connected with the nonresonance sound absorption, described in Eq. (11) by the functions $J_s^2 [k_H \rho \beta \sqrt{1 - p_H^2/p_{H \max}^2}]$.

In conclusion, we consider it our pleasant duty to express our sincere thanks to É. A. Kaner for numerous productive discussions of the present research and useful remarks, and also A. M. Grishin for great help in the interpretation of the experimental results.

¹⁾The single crystal of bismuth was grown in "Gidredmet."

- ¹A. B. Pippard, Phil. Mag. 2, 1147 (1957).
- ²V. L. Gurevich, Zh. Eksp. Teor. Fiz. 37, 71 (1959) [Sov. Phys. JETP 10, 51 (1960)].
- ³N. Mikoshiba, J. Phys. Soc. Japan 13, 759 (1958).
- ⁴É. A. Kaner, Zh. Eksp. Teor. Fiz. 43, 216 (1962) [Sov. Phys. JETP 16, 154 (1963)].
- ⁵M. Ya. Azbel', and É. A. Kaner, Zh. Eksp. Teor. Fiz. 30, 812 (1959); 32, 896 (1957) [Sov. Phys. JETP 3, 772 (1956); 5, 730 (1957)].
- ⁶T. Kjeldaas, Phys. Rev. 113, 1473 (1959).
- ⁷A. A. Galkin, E. A. Kaner and A. P. Korolyuk, Dokl. Akad. Nauk SSSR 134, 74 (1960); [Sov. Phys. Dokl. 5, 1004 (1961)]; Zh. Eksp. Teor. Fiz. 39, 1517 (1960) [Sov. Phys. JETP 12, 1055 (1961)].
- ⁸É. A. Kaner, V. G. Peschanskiĭ and I. A. Privorotskiĭ, Zh. Eksp. Teor. Fiz. 40, 214 (1960) [Sov. Phys. JETP 13, 147 (1961)].
- ⁹É. A. Kaner and V. L. Falko, Phys. Stat. Sol. 22, 319 (1967).
- ¹⁰A. P. Korolyuk and L. Ya. Matsakov, Zh. Eksp. Teor. Fiz. 52, 415 (1967) [Sov. Phys. JETP 25, 270 (1967)].
- ¹¹S. Hörenfeldt, Phys. Scripta 3, 45 (1971).
- ¹²J. A. Munarin, Phys. Rev. 172, 737 (1968).
- ¹³S. W. Hui and J. A. Rayne, J. Phys. Chem. Sol. 33, 611 (1972).
- ¹⁴J. D. Gavenda and B. C. Deaton, Phys. Rev. Lett. 8, 208 (1963).
- ¹⁵C. Burmeister, D. B. Doan and J. D. Gavenda, Phys. Lett. 7, 112 (1963).
- ¹⁶B. C. Deaton and J. D. Gavenda, Phys. Rev. 136A, 1096 (1964).
- ¹⁷Y. Eckstein, J. B. Ketterson and M. G. Priestley, Phys. Rev. 148, 586 (1966).
- ¹⁸V. S. Édel'man and M. S. Khaĭkin, Zh. Eksp. Teor. Fiz. 49, 107 (1965) [Sov. Phys. JETP 22, 77 (1966)].
- ¹⁹M. S. Khaĭkin and V. S. Édel'man, Zh. Eksp. Teor. Fiz. 49, 1695 (1965) [Sov. Phys. JETP 22, 1159 (1966)].
- ²⁰V. S. Édel'man, Zh. Eksp. Teor. Fiz. 64, 1734 (1973) [Sov. Phys. JETP 37, 875 (1973)].
- ²¹V. S. Édel'man, Zh. Eksp. Teor. Fiz. 68, 257 (1975) [Sov. Phys. JETP 41, 125 (1975)].
- ²²A. P. Korolyuk, V. F. Roĭ, A. V. Golik, L. Ya. Matsakov, V. I. Beletskiĭ and M. A. Obolenskiĭ, Prib. Tekh. Eksp. No. 4, 208 (1974).
- ²³A. A. Galkin and A. P. Korolyuk, PTE, No. 6, 99 (1960).
- ²⁴V. I. Beletskiĭ, A. V. Golik, L. Ya. Matsakova and A. P. Korolyuk, Prib. Tekh. Eksp. No. 5, 143 (1975).
- ²⁵A. P. Korolyuk, M. A. Obolenskiĭ and V. L. Fal'ko, Zh. Eksp. Teor. Fiz. 59, 377 (1970) [Sov. Phys. JETP 205 (1971)].
- ²⁶K. Walter, Phys. Rev. 174, 782 (1968).
- ²⁷A. P. Korolyuk, Zh. Eksp. Teor. Fiz. 49, 1009 (1965) [Sov. Phys. JETP 22, 701 (1966)].

Translated by R. T. Beyler